Electronic Annex

Combined mass-dependent and nucleosynthetic isotope variations in refractory inclusions and their mineral separates to determine their original Fe isotope compositions

Q.R. Shollenberger, A. Wittke, J. Render, P. Mane, S. Schuth, S. Weyer, N. Gussone, M. Wadhwa, and G.A. Brennecka

EA1 Fe isotope measurements and results

The reproducibility of our terrestrial rock standards BHVO-2 and BCR-2 are shown in Figs. EA1 and EA2 in comparison with literature data.

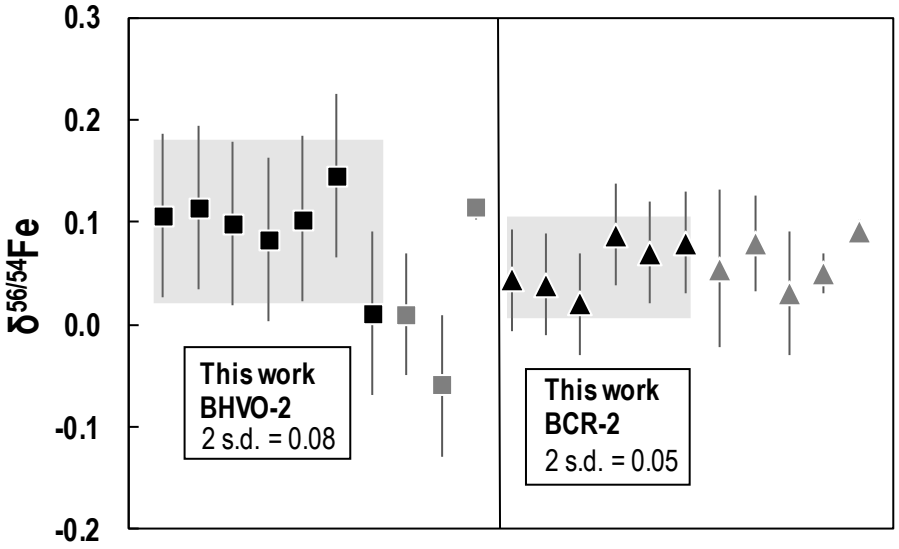

Figure EA1. Shown is a comparison of the $\delta^{56/54}$Fe values for terrestrial rock standards BHVO-2 and BCR-2 measured in this study (black symbols) along with literature data (grey symbols). Uncertainties of the samples and the grey shaded boxes are the 2SD of the respective rock standards. Literature data from: Dauphas et al., 2004; Weyer et al., 2005; Dideriksen et al., 2006; Craddock and Dauphas 2011; Schuth et al., 2015.

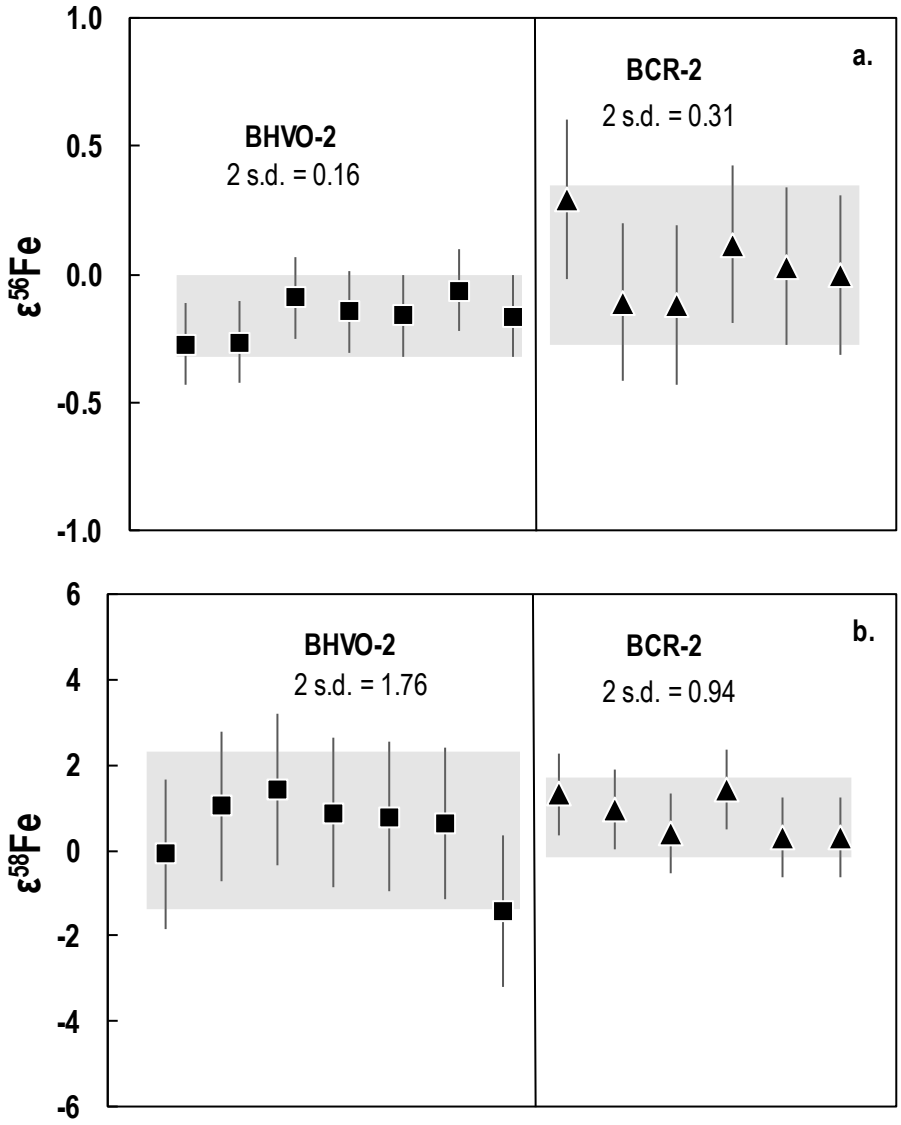

Figure EA2. Repeat analyses of the terrestrial rock standards BHVO-2 and BCR-2 throughout the measurement campaign for a) $\varepsilon^{56}Fe$ and b) $\varepsilon^{58}Fe$. Uncertainties of the samples and the grey shaded boxes are the 2SD of the respective rock standards. Data are internally normalized to $^{57}Fe/^{54}Fe = 0.36255$.

EA2 Location of Fe isotopic anomaly

In this study, we internally normalized our data to $^{57}Fe/^{54}Fe = 0.36255$ (Taylor et al., 1992). This normalization was selected because most Fe was produced in supernova explosions by radioactive ^{56}Ni decaying to ^{56}Fe (Clayton, 1999); thus, ^{56}Fe is important for isotopic investigation. Additionally, the least abundant isotope, ^{58}Fe (0.28%), is uniquely produced in a neutron-rich version of the equilibrium process in supernovae. As such, these two Fe isotopes are the most likely to preserve any signatures (Dauphas et al., 2004; Cook and Schönbächler, 2017).

EA3 Rare earth element data

Table EA1. Rare earth element data for the bulk CAIs and Egg 2 mineral separates normalized to CI using Lodders (2003).

	La	Ce	Pr	Nd	Sm	Eu	Gd	Tb	Dy	Ho	Er	Tm	Yb	Lu
AF01	234.69	192.16	235.29	247.77	225.32	33.00	199.91	176.93	156.17	50.19	20.03	189.36	17.88	9.89
AF02	4.38	3.95	4.33	4.48	4.34	1.56	2.05	1.56	1.14	0.35	0.18	3.83	0.89	0.12
AF03	3.20	2.58	3.44	3.39	3.22	5.88	2.09	1.70	1.53	0.82	0.65	5.28	2.92	0.38
AF04	31.85	39.72	35.71	35.14	37.72	11.94	13.64	11.59	9.00	2.51	1.68	33.96	8.94	1.16
Al01	18.95	17.30	16.40	17.07	15.89	13.54	16.96	15.87	16.68	15.09	15.60	14.10	14.90	15.49
Al02	24.07	25.75	25.14	19.80	18.80	7.59	7.13	5.72	4.92	2.83	2.39	12.04	5.61	1.70
A-ZH-2	17.43	17.89	15.87	15.68	15.53	19.44	17.05	15.92	16.98	16.16	16.76	16.33	15.26	16.59
A-ZH-3	14.09	14.07	13.40	13.33	13.55	20.46	14.02	12.98	13.70	13.23	13.79	13.57	14.43	13.73
A-ZH-4	13.70	13.38	12.67	12.48	12.59	16.29	13.62	12.57	13.30	12.96	13.66	12.42	12.89	13.93
A-ZH-5	15.55	15.56	15.21	15.38	15.76	5.31	16.16	15.13	15.84	15.30	15.90	15.69	10.63	15.90
CAI 164	7.67	8.10	8.29	8.46	8.90	9.61	8.06	8.82	8.57	8.45	8.93	8.44	10.01	9.20
CAI 165	5.78	4.97	6.10	6.47	6.27	4.41	5.22	5.81	5.72	5.72	5.98	5.30	3.24	5.93
CAI 166	22.44	23.83	24.23	24.77	25.76	4.21	14.54	13.53	10.21	2.38	0.87	20.59	0.84	0.23
CAI 167	20.20	18.75	21.16	21.33	21.39	3.14	9.11	8.02	5.69	1.64	1.08	14.75	2.06	0.72
CAI 168	8.40	8.67	8.80	8.96	9.24	10.86	8.40	9.11	8.91	8.90	9.61	8.62	9.93	10.19
CAI 170	12.56	12.33	12.78	12.05	13.30	15.81	12.50	14.44	13.82	13.52	13.76	14.78	14.77	12.91
CAI 171	12.50	14.36	14.33	13.09	14.17	10.25	10.12	12.07	13.19	19.63	22.83	15.62	7.51	22.58
CAI 172	21.99	21.34	23.15	22.49	24.97	31.02	24.99	28.65	28.35	28.64	30.38	27.79	31.57	28.85
CAI 173	19.53	17.44	20.54	20.31	21.92	9.74	20.33	24.25	23.64	22.56	23.24	21.92	8.43	20.25
CAI 174	28.65	27.07	27.44	25.99	28.16	36.49	26.51	31.84	31.79	31.97	34.24	31.17	36.24	33.30
CAI 175	52.89	44.12	51.23	50.67	45.95	4.41	39.43	42.11	35.20	14.35	7.61	42.23	4.94	1.58
Bart	23.64	23.10	24.75	26.71	28.24	22.34	29.43	29.62	29.31	27.87	28.24	27.79	17.62	25.00
Homer	6.87	6.76	6.50	6.28	6.08	2.59	1.69	1.46	1.14	0.61	0.57	5.19	4.78	0.54
Lisa	20.68	20.36	20.16	20.70	20.62	21.88	20.14	20.19	20.37	19.84	20.45	20.28	18.85	20.20
Marge	17.14	16.00	17.10	17.70	16.60	11.05	12.05	11.99	11.20	8.89	8.92	18.80	11.31	9.01
Egg 2 Plag	5.08	4.56	3.95	4.11	3.43	8.27	3.04	2.94	2.79	2.71	2.70	2.59	2.83	2.20
Egg 2 High-Mg Px	3.44	4.24	4.76	6.03	6.47	2.12	7.01	7.53	7.58	7.58	7.84	7.61	7.84	8.09
Egg 2 High-Fe Px	6.32	7.50	8.31	10.29	11.84	4.50	12.49	13.25	13.47	13.34	13.65	13.16	13.51	14.00

EA4 Concerns of incomplete sample digestion

One potential concern when investigating mass-dependent or non-mass-dependent isotope compositions is incomplete sample digestion which could produce spurious isotope results. Phases that are difficult to dissolve completely are spinel, chromite, and perovskite. However, most CAIs samples of this work were digested using either Parr Bombs or a high pressure acid digestion system which alleviates concern of incomplete sample digestion (Shollenberger et al., 2018; Brennecka et al., 2010). Samples from Burkhardt et al. (2008) and Kruijer et al. (2014) were digested on hot plates using very similar methodologies to one another (a combination of HF–HNO_3–$HClO_4$ followed by 6 M HCl–0.06 M HF) and both resulted in complete sample digestion which is described in detail in each manuscript. The Egg 2 mineral separates were dissolved at Arizona State University using a combination of concentrated HF, HNO_3, and HCl to completely dissolve the samples. Furthermore, the fact that the Egg 2 mineral separates have mass-dependent Ca isotope compositions and nucleosynthetic Ti, Ni, and Sr isotope anomalies consistent with literature data from other igneous CAIs (*e.g.*, Huang et al., 2012; Brennecka et al., 2013; Williams et al., 2016; Render et al., 2018) additionally alleviates the concern of incomplete sample digestion.

EA5 Concerns of previous chemical procedures

Some CAIs in this work had experienced previous ion-exchange procedures, providing a basis for possible isotope fractionation. However, as all previous column washes had been saved and recombined, resulting in high yields, there is a limited concern for mass-dependent isotopic fractionation from previous procedures. Column washes from previous chemical

procedures were dried down and stored in Teflon vials. These samples were redissolved in the appropriate acid and volume when sample solution aliquots were taken for Mg, Ca, Ni, and Fe isotope measurements.

Furthermore, the same CAIs were recently investigated for their Ni isotope compositions utilizing both unprocessed aliquots as well as sample aliquots which had seen previous ion chromatography (Render et al., 2018). For some of the exact same CAI samples, Render et al. (2018) showed indistinguishable Ni isotopic compositions for unprocessed aliquots and chemically processed aliquots (*e.g.*, CAI 164, CAI 165, CAI 168). Therefore, it is unlikely that any of the observed isotopic variations in our study are the result of isotope fractionation during chemistry. Note that the Fe sample solution aliquots were all taken prior to the Ni chemistry described in Render et al. (2018).

EA6 Correcting for mass-dependent and mass-independent effects

Previous work has shown that severe mass-dependent fractionation may result in spurious mass-independent effects (Render et al., 2018), as the exponential law is no longer valid. Given some of our samples have large mass-dependent effects in Fe, the ε^{56}Fe and ε^{58}Fe values from Table 4 have a second-order correction done for natural mass fractionation following Rayleigh distillation as shown by Render et al. (2018). Similar to Render et al. (2018), this correction was done by using the equations derived in Tang and Dauphas, (2012) but converting them into Fe isotope space. In this case, alpha is equal to the square root of the isotope masses. The specific equation is (2) from Tang and Dauphas, (2012) and is the following for ε^{56}Fe and ε^{58}Fe (n = –0.5):

$$\varepsilon^{56}Fe_{corr.} \approx 5 \times (–0.5–0)\ [(56\text{-}54)(56\text{-}57)/54]F \approx 0.093F$$

$$\varepsilon^{58}Fe_{corr.} \approx 5 \times (–0.5–0)\ [(58\text{-}54)(58\text{-}57)/54]F \approx –0.185F$$

where F is the Fe isotope fractionation in ‰/amu. As such, the corrected ε^{56}Fe and ε^{58}Fe are then:

$$\varepsilon^{56}Fe_{corr.} = \varepsilon^{56}Fe_{meas.} – (0.093F)$$

$$\varepsilon^{58}Fe_{corr.} = \varepsilon^{58}Fe_{meas.} – (–0.185F)$$

This correction utilizes the measured $\delta^{56/54}$Fe values for an individual sample. The propagated uncertainty on $\varepsilon^{56}Fe_{corr.}$ and $\varepsilon^{58}Fe_{corr.}$ depend strongly on the uncertainty of ε^{56}Fe and ε^{58}Fe. As such, the overall uncertainties are very similar to the uncertainties on ε^{56}Fe and ε^{58}Fe. See the supplement excel file where the calculations were performed. After this second-order correction, the Egg 2 mineral separates still had resolved ε^{56}Fe compositions. Given that Rayleigh fractionation would be the largest correction one could reasonably apply, it appears that the resolved ε^{56}Fe compositions are real and not an analytical artifact.

As the Egg 2 mineral separates have resolved ε^{56}Fe compositions, their $\delta^{56/54}$Fe compositions were corrected for the anomaly on ^{56}Fe (this was also done for A-ZH-1 which hinted at a ^{56}Fe anomaly). This was done by subtracting the $\varepsilon^{56}Fe_{corr.}$ anomaly from the measured $\delta^{56/54}$Fe composition.

EA7 Ni isotope measurements of the Egg 2 separates

Previous work has demonstrated that Ni isotope measurements can be affected by Zn interferences, particularly ^{64}Zn on ^{64}Ni (Tang and Dauphas, 2012; Render et al., 2018), and

Render et al. (2018) discarded any measurements with Zn/Ni > 1.5×10^{-4}. Importantly, the Egg 2 high-Fe Px had a Zn/Ni of 3.2×10^{-4}, which is just outside the threshold used in Render et al. (2018). However, previous work has demonstrated with Zn doping tests that interferences from ^{64}Zn can be accurately corrected with Zn/Ni < 9.5×10^{-4} (Tang and Dauphas, 2012; Render et al., 2018). Therefore, regardless of the small amount of Zn present during the Egg 2 high-Fe Px measurement, we are confident in the reported ε^{64}Ni value of 2.25 ± 0.60 within its given uncertainty.

EA8 Concern of an analytical artifact for ε^{56}Fe vs. $\delta^{56/54}$Fe

The observed correlation between mass-independent and mass-dependent Fe isotope compositions should be evaluated carefully as such a correlation is unexpected. However, as described in section EA6, the mass-independent data has been corrected using a previously derived equation for this exact purpose and mass-dependent results have also been corrected for mass-independent effects. After these corrections, a correlation is still present in our samples (Fig. 9). Importantly, mass-dependent fraction can occur 1) in nature, 2) during separation and purification, and 3) during mass spectrometry. We have very high confidence that any mass-dependent fractionation during mass spectrometry is accurately corrected in this work. The details regarding Fe isotope measurement using Cu-doping have been well-documented (*e.g.*, Arnold et al., 2004) and all of our samples plot along linear trends with the expected slopes (Fig. EA3). Regarding the chemical separation and purification, our terrestrial rock standards and a measurement of bulk Allende have unresolved $\delta^{56/54}$Fe, ε^{56}Fe, and ε^{58}Fe compositions, in agreement with previous work (*e.g.*, Völkening and Papanastassiou, 1989; Weyer et al., 2005; Dauphas et al., 2004; Tang and Dauphas, 2012). Furthermore, for each Egg 2 mineral separate, two sample solution aliquots were taken and processed through the chemical procedures and measured during two different analytical sessions. The results from both sessions give consistent results. Regarding mass-dependent fractionation in nature, the second-order correction described in section EA6 should account for this. As such, the correlation between mass-independent and mass-dependent Fe isotope compositions likely represents a mixing line as described in the main text (sections 4.3.2).

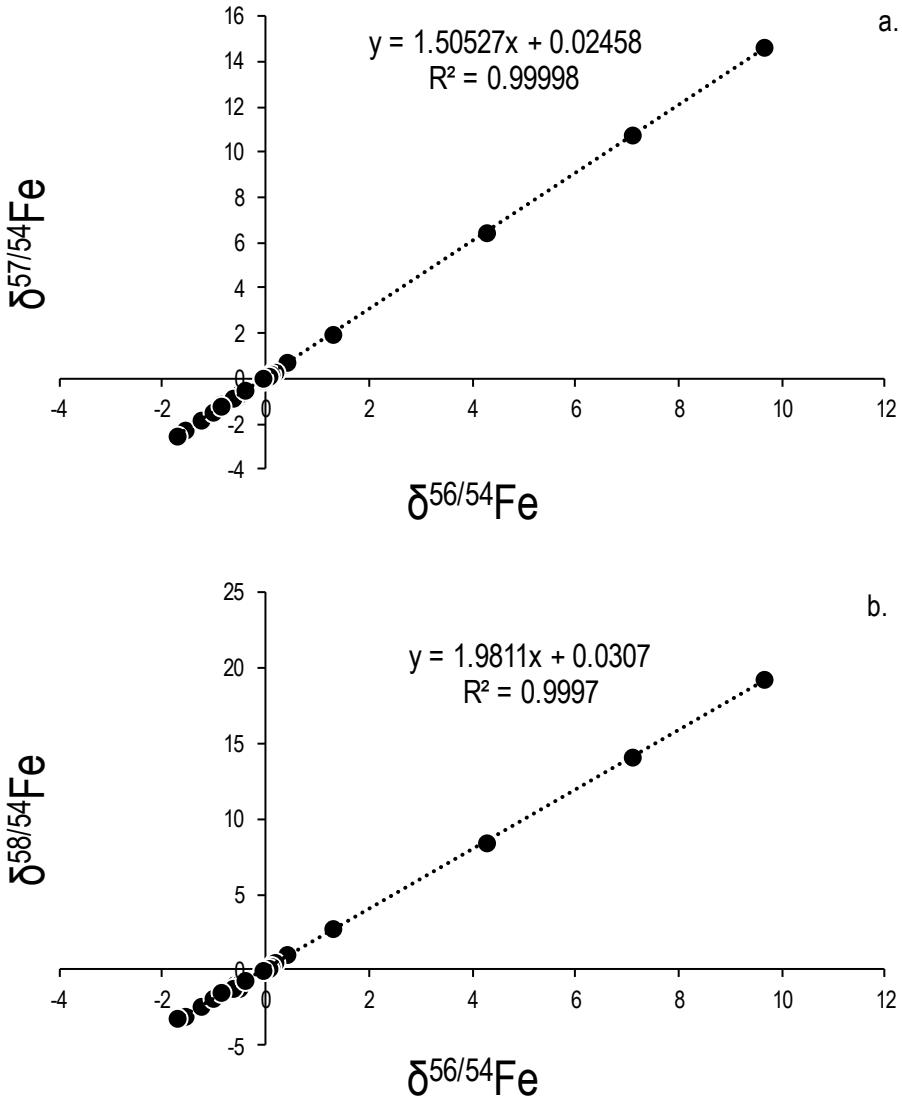

Figure EA3. a) $\delta^{57/54}$Fe vs. $\delta^{56/54}$Fe and b) $\delta^{58/54}$Fe vs. $\delta^{56/54}$Fe for all samples during this work using Cu-doping to correct for instrumental mass bias. The samples plot along well-defined correlation lines.

References

Arnold G.L., Weyer S., and Anbar A.D. (2004) Fe isotope variations in natural materials measured using high mass resolution multiple collector ICPMS. *Anal. Chem.* **76**, 322-327.

Brennecka G.A., Weyer S., Wadhwa M., Janney P.E., Zipfel J., and Anbar A.D. (2010) ^{238}U/^{235}U Variations in Meteorites: Extant ^{247}Cm and Implications for Pb-Pb Dating. *Science* **327**, 449-451.

Brennecka G.A., Borg L.E., and Wadhwa M. (2013) Evidence for supernova injection into the solar nebula and the decoupling or r-process nucleosynthesis. *Proc. Nat. Acad. Sci.* **110**, 17241-17246.

Burkhardt C., Kleine T., Bourdon B., Palme H., Zipfel J., Friedrich J.M., and Ebel D.S. (2008) Hf-W mineral isochron for Ca,Al-rich inclusions: Age of the solar system and the timing of core formation in planetesimals. *Geochim. Cosmochim. Acta* **72**, 6177-6197.

Clayton D.D. (1999) Radiogenic iron. *MAPS* **34**, A145-A160.

Cook D.L. and Schönbächler M. (2017) Iron isotopic compositions of troilite (FeS) inclusions from iron meteorites. *The Astronomical Journal* **154**, 172-179.

Craddock P.R. and Dauphas N. (2011) Iron isotopic compositions of geological reference materials and chondrites. *Geostandards & Geoanalytical Research* **35**, 101-123.

Dauphas N., Janney P.E., Mendybaev R.A., Wadhwa M., Richter F.M., Davis A.M., van Zuilen M., Hines R., and Foley C.N. (2004) Chromatographic separation and multicollection-ICPMS analysis of iron. Investigating mass-dependent and -independent isotope effects. *Anal. Chem.* **76**, 5855-5863.

Dideriksen K., Baker J.A., and Stipp S.OL.S. (2006) Iron isotopes in natural carbonate minerals determined by MC-ICPMS with a ^{58}Fe-^{54}Fe double spike. *Geochim. Cosmochim. Acta* **70**, 118-132.

Huang S., Farkaš J., Yu G., Petaev M.I., and Jacobsen S.B. (2012) Calcium isotopic ratios and rare earth element abundances in refractory inclusions from the Allende CV3 chondrite. *Geochim. Cosmochim. Acta* **77**, 252-265.

Kruijer T.S., Kleine T., Fischer-Gödde M., Burkhardt C., and Wieler R. (2014) Nucleosynthetic W isotope anomalies and the Hf-W chronometry of Ca-Al-rich inclusions. *Earth Planet. Sci. Lett.* **403**, 317-327.

Lodders K. (2003) Solar system abundances and condensation temperatures of the elements. *Astrophys. J.* **591**, 1220-1247.

Render J., Brennecka G.A., Wang S., Wasylenki L.E., and Kleine T. (2018) A distinct nucleosynthetic heritage for early Solar System solids recorded by Ni isotope signatures. *Astrophys. J.* **862**, 1-18.

Schuth S., Hurraß J., Münker C., and Mansfeldt T. (2015) Redox-dependent fractionation of iron isotopes in suspensions of a groundwater-influenced soil. *Chem. Geol.* **392**, 74-86.

Shollenberger Q.R., Borg L.E., Render J., Ebert S., Bischoff A., Russell S.S., and Brennecka G.A. (2018) Isotopic coherence of refractory inclusions from CV and CK meteorites: Evidence from multiple isotope systems. *Geochim. Cosmochim. Acta* **228**, 62-80.

Tang H. and Dauphas N. (2012) Abundance, distribution, and origin of ^{60}Fe in the solar protoplanetary disk. *Earth Planet. Sci. Lett.* **248**, 248-263.

Taylor P.D.P., Maeck R., and De Bievre P. (1992) Determination of the absolute isotopic composition and atomic weight of a reference sample of natural iron. *Int. J. Mass Spectrom. Ion Processes* **121**, 111-125.

Völkening J. and Papanastassiou D.A. (1989) Iron isotope anomalies. *ApJ* **347**, L43–L46.

Weyer S. Anbar A.D., Brey G.P., Münker C., Mezger K., and Woodland A.B. (2005) Iron isotope fractionation during planetary differentiation. *Earth Planet. Sci. Lett.* **240**, 251-264.

Williams C. D., Janney P. E., Hines R. R., and Wadhwa M. (2016) Precise titanium isotope compositions of refractory inclusions in the Allende CV3 chondrite by LA-MC-ICPMS. *Chem. Geol*. **436**, 1-10.